NASA TECHNICAL NOTE

NASA TN D-8336

NASA TN D-8336 c.1

GENERALIZATION AND REFINEMENT OF AN AUTOMATIC LANDING SYSTEM CAPABLE OF CURVED TRAJECTORIES

Windsor L. Sherman

Langley Research Center
Hampton, Va. 23665

NATIONAL AERONAUTICS AND SPACE ADMINISTRATION • WASHINGTON, D. C. • NOVEMBER 1976

Completed 13 Apr 77
lm

ERRATA

NASA Technical Note D-8336

GENERALIZATION AND REFINEMENT OF AN AUTOMATIC LANDING SYSTEM CAPABLE OF CURVED TRAJECTORIES

Windsor L. Sherman
November 1976

Replace page 17 with the attached page 17.

Issued March 1977

1. Report No.	2. Government Accession No.	3. Recipient's Catalog No.
NASA TN D-8336		

4. Title and Subtitle	5. Report Date
GENERALIZATION AND REFINEMENT OF AN AUTOMATIC LANDING SYSTEM CAPABLE OF CURVED TRAJECTORIES	November 1976
	6. Performing Organization Code
7. Author(s)	8. Performing Organization Report No.
Windsor L. Sherman	L-10686
	10. Work Unit No.
9. Performing Organization Name and Address	505-06-93-04
NASA Langley Research Center Hampton, VA 23665	11. Contract or Grant No.
	13. Type of Report and Period Covered
12. Sponsoring Agency Name and Address	Technical Note
National Aeronautics and Space Administration Washington, DC 20546	14. Sponsoring Agency Code

15. Supplementary Notes

16. Abstract

Refinements in the lateral and longitudinal guidance for an automatic landing system capable of curved trajectories have been studied. Wing flaps or drag flaps (speed brakes) were found to provide faster and more precise speed control than autothrottles. In the case of the lateral control, it is shown that the use of the integral of the roll error in the roll command over the first 30 to 40 seconds of flight reduces the sensitivity of the lateral guidance to the gain on the azimuth-guidance-angle error in the roll command. Also, changes to the guidance algorithm are given that permit π-radian approaches and constrain the airplane to fly in a specified plane defined by the position of the airplane at the start of letdown and the flare point.

17. Key Words (Suggested by Author(s))	18. Distribution Statement
Guidance Terminal area Landing	Unclassified - Unlimited Subject Category 04

19. Security Classif. (of this report)	20. Security Classif. (of this page)	21. No. of Pages	22. Price*
Unclassified	Unclassified	36	$3.75

* For sale by the National Technical Information Service, Springfield, Virginia 22161

GENERALIZATION AND REFINEMENT OF AN AUTOMATIC LANDING SYSTEM CAPABLE OF CURVED TRAJECTORIES

Windsor L. Sherman
Langley Research Center

SUMMARY

Refinements in the lateral and longitudinal guidance for an automatic landing system capable of curved trajectories have been studied. Wing flaps or drag flaps (speed brakes) were found to provide faster and more precise speed control than autothrottles. In the case of the lateral control, it is shown that the use of the integral of the roll error in the roll command over the first 30 to 40 seconds of flight reduces the sensitivity of the lateral guidance to the gain on the azimuth-guidance-angle error in the roll command. Also, changes to the guidance algorithm are given that permit π-radian approaches and constrain the airplane to fly in a specified plane defined by the position of the airplane at the start of letdown and the flare point.

INTRODUCTION

An automatic landing system capable of guiding an airplane to a precise landing would be of distinct benefit to both civil and military aircraft operations, as the cessation of operations due to inclement weather would be greatly reduced, as would the use of alternate airfields, which are often a long distance from the original destination. Reference 1 describes and reports the performance in a bland environment of an automatic landing system that can guide an airplane along a steep, curved trajectory to a precise landing without the use of a nominal trajectory. Reference 2 considers the same system in a nonbland environment. The disturbances considered were wind, wind shears, turbulence, data sample rate, and control-surface-actuator natural frequencies. Data rate compatibility with the microwave landing system was shown.

The work reported herein generalizes the basic system described in references 1 and 2 so that the guidance commands can be generated from data acquired by ground-based acquisition systems. Constraints on the flight-path angle and the use of aerodynamic surfaces instead of automatic throttles for speed control are investigated. Modifications to the lateral guidance system that remove the sensitivity of lateral guidance to the gain on the runway centering error are given. Unless otherwise noted, all data presented herein were obtained with a steady wind and the patchy turbulence described in reference 2.

SYMBOLS

The International System of Units is used throughout this paper. All angles are measured in radians.

D	operator, $\frac{d}{dt}$
g	acceleration due to gravity
h	altitude
k_{IG}	integration gain in lateral guidance
$k_1 \ldots k_{19}$	gains
m	mass
q	pitch rate
R	range, slant distance from ground data station to airplane, positive from airplane to radar
R_H	projection of R in horizontal plane
R_{11}	component of R_H parallel to runway center line
R_{12}	component of R_H perpendicular to runway center line
R_{13}	component of R in vertical plane
T	thrust
t	time
$\dot{u}$	acceleration in x body direction
u_w, v_w, w_w	windspeeds along x-, y-, and z-axes, respectively
V_c	speed command
V_T	speed in inertial space
w_{z_j}	vertical touchdown speed
X,Y,Z	inertial axes
x	$\blacksquare R_{11} - 900.0$
x,y,z	coordinates

α angle of attack

γ flight-path angle

δ_f flap deflection

δ_{SB} speed-brake deflection

ϵ_f flap angle change

ζ_1 runway coordinate, positive from landing point to opposite end of runway

ζ_2 runway coordinate, positive to right of runway

θ pitch attitude

θ_A radar azimuth angle

θ_{AA} actual azimuth guidance angle

θ_{AC} command azimuth guidance angle

θ_e radar elevation angle

ξ $= \tan^{-1}\left(\frac{h - 20}{R_{11} - 1175}\right)$

τ servo time constant

ϕ roll angle

ψ heading angle

Subscripts:

c command

i initial

o output

p plane

A dot over a variable indicates differentiation with respect to time.

BASIC AUTOLAND SYSTEM

The autoland system used in this study is the system described in reference 1, modified for the effect of wind as described in reference 2. In the system described in references 1 and 2, an airborne radar was assumed

and modeled as part of the system. Actually, the only data needed are the components of the range and range-rate vectors along and perpendicular to the runway center line. It was assumed that the airplane would be supplied with that data. Several methods of using these data in an airborne processor to obtain the inputs to the guidance laws are:

(1) Use range data to obtain ψ, θ_{AC}, θ_{AA}, and γ_c.

(2) Use range data to obtain θ_{AC}, θ_{AA}, and obtain γ_c and ψ from an inertial measuring unit.

(3) Use the range and range-rate data to obtain ψ, θ_{AC}, θ_{AA}, and γ_c.

The first method was discarded because small differences of large numbers were involved in the determination of ψ. The second method is essentially the one used in reference 2. The third method was used to obtain the data for the guidance laws in this paper. It was assumed that the three components of range and range rate R_{11}, R_{12}, R_{13} and $\dot{R}_{11}$, $\dot{R}_{12}$, and $\dot{R}_{13}$, respectively, were supplied to the airplane guidance system. The equations used to determine the information for the guidance laws were

$$R_H = \sqrt{R_{11}^2 + R_{12}^2} \tag{1}$$

$$R = \sqrt{R_{11}^2 + R_{12}^2 + R_{13}^2} \tag{2}$$

$$\dot{R}_H = \sqrt{\dot{R}_{11}^2 + \dot{R}_{12}^2} \tag{3}$$

$$\dot{R} = \sqrt{\dot{R}_{11}^2 + \dot{R}_{12}^2 + \dot{R}_{13}^2} \tag{4}$$

$$\theta_A = \sin^{-1}\left(R_{12}/R_H\right) \tag{5}$$

$$\theta_e = \tan^{-1}\left(R_{13}/R_H\right) \tag{6}$$

(See fig. 1.) The heading angle of the airplane was calculated by using an inverse tangent method based on the sine and cosine so that the correct quadrant was obtained. The equations used were

$$\sin \psi = \dot{R}_{12}/\dot{R}_H \tag{7}$$

$$\cos \psi = \dot{R}_{11}/\dot{R}_H \tag{8}$$

and the heading angle was obtained from

$$\psi = \tan^{-1}(\sin \psi/\cos \psi) \tag{9}$$

This is equivalent to determining ψ from $\tan^{-1}\left(\dot{R}_{12}/\dot{R}_{11}\right)$ because the inverse tangent is defined only between 0 and $\pm\pi/2$. The use of equations (7) to (9) removes ambiguity as to the proper quadrant for the angle ψ. The other data were calculated as follows

$$\theta_{AA} = \theta_A - \psi \tag{10}$$

$$\theta_{AC} = \tan^{-1}\left(\frac{100.0}{R_H \cos \theta_{AA}}\right) \tag{11}$$

If the initial heading angle ψ_i is greater than $\pi/2$, the angle θ_{AA} passes through $\pi/2$ during the landing maneuver. This causes the tangent of θ_{AC} to become infinite and large roll angles are commanded. Therefore, if ψ_i was greater than $\pi/2$, θ_{AC} was calculated by the alternate expression

$$\theta_{AC} = \tan^{-1}\left(\frac{100.0}{R_H}\right) \tag{12}$$

throughout the landing maneuver. In addition to the angles θ_{AA} and θ_{AC}, the commanded letdown γ_c and the flight-path angle of the airplane γ were needed for the vertical guidance. These were given by

$$\gamma_c = -\tan^{-1}\left[\frac{R_{13} - 20}{\sqrt{(R_{11} - 1175)^2 + R_{12}^2}}\right] \qquad (H > 20.0) \tag{13}$$

$$\gamma_c = -\tan^{-1}\left(\frac{R_{13}|\tan \gamma_{20}|}{20.0}\right) \qquad (H < 20.0) \tag{14}$$

where γ_{20} is the value of the airplane flight-path angle at an altitude of 20 meters. The flight-path angle of the airplane was determined by the use of the expression

$$\gamma = -\tan^{-1}\left(\dot{R}_{13}/\dot{R}_H\right) \tag{15}$$

The quantities θ_{AC}, θ_{AA}, and ψ given by equations (9) to (12) were used in the turn algorithm, which is

$$\phi_c = k_2\left[\psi_c - \psi - k_3\dot{\psi} + k_1\left(\theta_{AC} - \theta_{AA}\right)\right] \tag{16}$$

where ψ_c is the heading of the runway and the gains k_1 and k_2 were calculated by the method given in appendix B of reference 2 and k_3 is a constant gain and is equal to 0.8. The quantities γ_c and γ, given by equations (13), (14), and (15), were used in the letdown algorithm to generate a pitch-rate command for the autopilot. The algorithm, given in reference 1, is

$$q_c = -k_5\left[k_{14}\left(\gamma_c - \gamma_o\right) + \frac{g \tan \phi_c}{V_T} \sin \phi_c + \dot{\alpha}\right] - k_{16}\int_0^t \left(\gamma_c - \gamma_o\right)dt \tag{17}$$

The gains and conditions on the use of the letdown algorithm are given in appendix E of reference 1.

Winds and Turbulence Used in Study

Steady wind and turbulence were used in most cases presented in this paper. In the program used to generate the wind and turbulence, headwinds

were negative and down blasts were positive. The steady windspeed was -25.8 m/sec and was directed at $\pi/4$ radians to the runway center line so there was a component of -18.24 m/sec along the runway and -18.24 m/sec across the runway. There was no vertical component of the steady wind. The turbulence was based on the output of a random number generator that gave a normal distribution of random numbers between ±1. The specific turbulence used was the patchy turbulence used in reference 2. The turbulence was calculated along all three inertial axes, then summed with the steady wind components and transformed to airplane axes for use in the calculations. The turbulence generated along each axis is shown in figure 2 and covers 120 seconds of flight time. As the turbulence is the same from run to run, these curves show the turbulence the airplane is experiencing as it makes the landing maneuver.

Acceptable Touchdown Conditions

In the investigation reported herein, the landing was assumed to take place on a runway 3000 meters long and 50 meters wide. The desired touchdown point was on the center line 100 meters from the threshold of the runway. The values of θ, ψ, ζ_1, ζ_2, and γ, because of the reference used, indicate the errors from the ideal touchdown condition in which all these variables would have a value of zero. For the purpose of determining whether a landing was satisfactory, an arbitrary set of conditions was established. If a landing fitted within the following limits, it was said to be satisfactory:

$\phi = \pm 0.06$ rad

$\psi = \pm 0.01$ rad

$\zeta_1 = 0$ to 500 m from touchdown point

$\zeta_2 = \pm 10$ m

$0 > \gamma_o \geqq -1.98 \times 10^{-2}$ rad

$0 < w_{z_j} \leqq 1.0$ m/sec

$0.017 \leqq \theta \leqq 0.061$ rad

The angle ψ gives the direction of the velocity vector when wind and turbulence are present or the direction of the airplane x-axis when there is no wind nor turbulence. It is always referred to as the heading angle.

RESULTS AND DISCUSSION

Autoland Longitudinal Control

The longitudinal control of the basic system described in references 1 and 2 is achieved by the following three subsystems:

(1) The flight-path control system - this system receives guidance information from the guidance computer and controls the letdown of the airplane to the runway and, working with the sideslip control, provides turn coordination.

(2) The automatic trim system - this system makes use of the stabilizer to trim continuously the pitching moment due to angle of attack.

(3) The speed-control system - this system uses automatic throttles to control the speed of the airplane to specified values of approach speed and landing speed that are contained in the guidance computer and fed to the speed-control system as a function of flight-path angle and altitude.

These three systems operated in combination to provide adequate automatic longitudinal control for the autoland system. Speed regulation was poor but sufficient for the landing maneuver.

The results of further investigations on the flight-path and speed-control systems that improve the response of these systems and constrain the flight path to a specified plane are presented in the following sections. The flight-path control system is discussed first.

Flight-path control system.- The flight-path control system used in references 1 and 2 is essentially the same system. When a vertical displacement occurs as the result of wind or turbulence, the guidance does not attempt to return the airplane to the previous flight path, but it determines a new letdown strategy so that the airplane can fly to the landing point from its present position.

Gain changes and flap settings.- Further investigation showed that improved performance could be obtained by making minor modifications to the basic system. These modifications are to replace the term $\dot{\alpha}$ with $\dot{\alpha} \sin \phi_c$ and to change k_{16} from 1.0 to 0.8 in equation (17). In addition to these gain studies, it was found that lowering the upper limit on flap deflection helped the airplanes attain a proper pitch attitude for landing (ref. 1). In still air, limiting the deflection to 0.61087 radian improved the pitch altitude from -2.25×10^{-2} radian to 4.79×10^{-2} radian. Thus, limiting the flap deflection changed an unacceptable pitch attitude to an acceptable one. The maximum flap deflection was found to vary with windspeed. For a wind of -25.8 m/sec (headwind) at 0.7584 radian to the runway center line the flap deflection used was 0.2618 radian so as to achieve a pitchup attitude at touchdown. As this wind vector was the only one used, the exact variation of the maximum flap setting with wind is not known.

Letdown-system constraints.- The letdown system used in the basic autoland system is constrained so that letdown does not start until the flight-path-angle command at the start of a landing maneuver is greater than -0.073 radian. The airplane maintains constant altitude flight until the letdown conditions are met. The ability of this system to hold altitude while making turns was demonstrated in reference 1. The introduction of winds and turbulence did not alter this ability. Flight-path-angle constraints up to -0.10472 radian have been used successfully.

A flight-path constraint that forces the system to control the flight path to a specified plane was also investigated. Note that the flight-path constraint selected is only one of a number of possible constraints; for instance, a curve surface could have been used. The flight-path constraint used was selected because it was thought to be more generally applicble than the others.

The plane used is defined by two lines that are perpendicular to the plane defined by the runway center line and the vertical to it. The first line passes through the present position of the airplane, and the second through the start-of-flare point. (See fig. 3.) The slope of the plane is given by

$$\xi = \tan^{-1}\left(\frac{h - 20}{R_{11} - 1175}\right) \tag{18}$$

The angle ξ is continuously calculated until it is equal to a predetermined value of γ called γ_p. When $\xi = \gamma_p$, letdown starts and γ_c is calculated by the formula

$$\gamma_c = \gamma_p \cos \psi \tag{19}$$

where ψ is the heading angle of the velocity vector with respect to the runway center line. The use of the heading angle in γ_c as a cosine function is so that the airplane decreases its flight-path angle as it turns towards the perpendicular to the runway center line.

In addition to equations (18) and (19), a logic block is necessary for those cases that have an initial heading angle greater than $\pi/2$ radians. This logic holds $\gamma_c = 0$ and prevents the calculation of ξ (eq. (18)) until $\dot{R}_{11} < 0$ and $\psi \leq \pi/2$.

The altitude time history, altitude track, and ground track for a plane-constrained letdown are shown in figure 4. The ground track (fig. 4(c)) is the usual ground track for this initial condition, which is $\zeta_1 = -3000.0$ meters, $\zeta_2 = -4000.0$ meters, $h = 200$ meters, and $\psi_i = 0.0$. Wind and turbulence were not used in this case. Two curves are shown for the altitude track and altitude time history. The curve with the plus marks is the desired flight path, and the unmarked curve is the actual flight path. The plus marks are also time marks and are spaced at 5-second intervals. As can be seen, the airplane when letting down is actually flying slightly above the desired flight path. This type of flight is acceptable as it is better to fly slightly above the glide slope than below it. In addition to the change in γ_c it was necessary to change the gain k_{16} in equation (17) from 1.0 to 2.1. The touchdown conditions for this case are

$$\phi = -4.72 \times 10^{-2} \text{ rad}$$

$$\psi = 1.895 \times 10^{-2} \text{ rad}$$

$$\zeta_2 = -2.624 \text{ m}$$

$V_T = 69.89$ m/sec

$\theta = 3.09 \times 10^{-2}$ rad

$\zeta_1 = 2.83 \times 10^{2}$ m

$\gamma = -8.761 \times 10^{-4}$ rad

$w_{z_j} = 0.061$ m/sec

and all are within acceptable limits. Figure 5 shows the altitude time history and altitude track for plane-constrained flight at the same initial condition when wind and turbulence were added to the simulation. There was no discernible alteration in the ground track. Even in the heavy wind and turbulence used in this problem the system was able to control the flight path to within reasonable limits of the desired flight. The large excursion that starts at about 68 seconds is caused by the airplane entering a region of heavy horizontal turbulence and down blasts. (See fig. 2.) In spite of the severity of the turbulence the system was able to maintain control of the airplane and effect a reasonable landing. The touchdown conditions for this case are

$\phi = 1.391 \times 10^{-2}$ rad

$\psi = 1.534 \times 10^{-1}$ rad

$\zeta_2 = 1.177 \times 10^{1}$ m

$V_T = 7.421 \times 10^{1}$ m/sec

$\theta = 2.775 \times 10^{-3}$ rad

$\zeta_1 = 9.873$ m

$\gamma = -1.446 \times 10^{-2}$ rad

$w_{z_j} = 1.073$ m/sec

Three touchdown conditions ψ, ζ_2, and w_{z_j} are unacceptable. The cause of ψ and ζ_2 not meeting standards is probably the turbulence that hit the airplane at 60 seconds. As the landing took place 11 seconds after the onset of the extreme turbulence, little time was available to recover and correct path fluctuations caused by the turbulence. The condition w_{z_j} is 1.073 m/sec above the largest permissible value. This excess vertical speed is attributed to the down blasts and poor speed-control system. The speed was about 7.0 m/sec above the commanded value of 67 m/sec. If the commanded value had been met, w_{z_j} would have been below the maximum permissible value for this parameter.

Speed-control system.- The details of the original speed-control system are given in appendix A. As indicated in appendix A, the gain k_{15} has a value of 1.0. The curve labeled A in figure 6 shows the speed regulation obtained with this system (see table I) in still air. The initial speed was 77.12 m/sec and, as soon as the airplane started to let down, between 0.0 and 1.0 second, a speed change to 72.43 m/sec was given. At about 40 seconds the speed entered the dead band of ±1.0 m/sec and remained within the dead band until a new speed command of 67.0 m/sec was introduced at about 73 seconds. The control system was never able to bring the speed to within ±1.0-m/sec dead band around the new command speed. The root-mean-square (rms) error in speed from 0 to 73 seconds was 3.12 and from 73 seconds on was 3.11. Curve B shows the effect of reducing the gain k_{15} to 0.45. The dead band was achieved at about 40 seconds but the large overshoot at the beginning followed by the undershoot caused the rms error to increase to 3.52. However, better speed regulation was achieved. The dead band was achieved 2 seconds before touchdown, the end of the trace. In this case the rms error for regulation around 67 m/sec was 2.83. In spite of the poorer rms error over the first part of curve B, it was considered more acceptable than curve A because of the better speed control over the critical final part of the run. The landing conditions for the runs from which curves A and B were abstracted were acceptable. The speed response when wind and turbulence were added (see table I) is shown as curve C in figure 6. In this case, the speed never enters and holds within the ±1-m/sec dead band, and the time represented is shorter because the airplane landed short of the touchdown point. Because the excursions from the commanded velocity are less than in other cases at the beginning of the run, the rms error over the first 74 seconds is slightly smaller, 2.98; however, from that point to the end of the run the rms error is 7.80.

Because of the poor response of jet engines to calls for thrust changes and because further changes in k_{15} give no significant improvement in speed response, it was decided to investigate the use of aerodynamic surfaces as speed-control devices.

Pure drag surfaces.- The first type of surface to be considered for speed control was a pure drag surface or speed brake. When this surface was used, the airplane was trimmed with the speed brakes undeflected. Deflections of the speed brakes were used to control the speed of the airplane by changing the deflection angle of the speed-brake panels. It was assumed that the speed brakes were flat plates with a drag coefficient of 1.0 when they were deflected perpendicular to the plane of symmetry of the airplane. For intermediate settings it was assumed that the drag coefficients varied directly as the sine of the deflection angle. Details of the system used to control these speed brakes are given in appendix B. The ability of the drag flaps to control the speed of the airplane is compared with that of the automatic throttle in figure 7. The automatic-throttle speed control is represented by curve C and the drag flaps by curve D. Over the first 74 seconds the rms error for the drag flap was 1.12 as compared with 2.96 for the automatic throttle. During the time from 74 seconds to touchdown, the rms errors were 2.42 and 7.80, respectively. The touchdown conditions for drag flaps were acceptable except for the vertical touchdown speed, which was marginal at 1.39 m/sec. This higher than acceptable touchdown speed proba-

bly results from the high turbulence that occurred from 68 to 77 seconds. A comparison of curves C and D of figure 7 shows that the drag flaps provide faster and more precise control of the speed than do the automatic throttles. However, in order to accomplish the speed regulation, the drag flaps had to provide, based on wing area, an increase of 0.11 in the drag coefficient. Under the assumptions concerning the drag flaps, this means that the drag flaps would have to have an area equivalent to the area of the wing flaps. Because of the size equivalence it was decided to investigate the use of wing flaps as a speed-control device.

Wing flaps.- Except for the change in constants (see appendix B), the control system used for the wing flaps was the same as that used for the drag flaps. The wing flaps were at an initial deflection of $\pi/12$ radians and the thrust trimmed. This thrust was then held constant throughout the landing maneuver. The speed regulation obtained from the use of wing flaps is compared with that obtained from automatic throttles in figure 7. Curve E is for the wing flaps and curve C is for the automatic throttle. The rms over the first 74 seconds was 0.51 for wing flaps and 2.96 for the autothrottle. Over the critical final part of the landing maneuver, the rms errors were 1.58 and 7.80, respectively, for the wing flaps and automatic throttles. The rms error in speed obtained for the wing flaps represents an improvement over that obtained for the speed brakes. The wing-flap speed-control touchdown conditions given in table I are within acceptable limits. An examination of the accelerations along the x body axis of the airplane showed that the maximum acceleration was -0.22 g unit (1g = 9.80665 m/sec^2) and occurred just after the speed change commands were given. This acceleration is a little high for passenger comfort but could be reduced by restricting the flap-deflection rate. The most significant difference is the time taken by the speed brakes to reduce the speed after a command was given. The speed-reduction commands occurred at points 0.001 second and at 74 seconds. After the first command, it took the speed brakes 14 seconds to achieve a speed level that the wing flaps achieved in 4 seconds. After the second speed command, the speed brakes were not able to reduce the speed to 67 m/sec before touchdown, whereas the wing flaps were able to reduce the speed to 67 m/sec in 6 seconds. The delay in speed regulation associated with the speed brakes at the start of the landing maneuver is tolerable, as it occurs far from touchdown and between 14 and 74 seconds. Differences in speed regulation are negligible. However, the delay in achieving 67 m/sec is more critical, as it occurs during the last few seconds of flight.

The motions of the speed brakes and wing flaps, when used to control speed, are about the same; both are responding to turbulence. See figures 8 and 9 for time histories of the speed-brake and wing-flap motions. The most erratic motion occurs around 70 seconds when the turbulence is most severe. Although the motions are equally erratic, the damping gain required with speed brakes was about 2.5 times that required for wing flaps.

The results obtained from the three methods of speed control, autothrottle, speed brakes, and wing flaps, indicate that wing flaps, because of the precise speed control, constitute the most desirable method.

Wing-flap speed control was tried for other wind conditions than those given in this section. The speed control was equally good under all conditions investigated, but it was found that flap-deflection angles had to be increased so as to obtain good speed regulation from a windspeed of 25.80 m/sec to zero windspeed.

Effect of speed control on touchdown conditions.- An examination of the touchdown conditions for the various methods of speed control given in table I shows that case E has the best touchdown conditions of the group. The ground tracks for cases C and E are shown in figure 10. The only difference between the systems that produced the ground tracks is the method of speed control. When wing-flap speed control is used, the first turn is tighter and this influences the ground track and letdown. Note that curve E alines with the runway sooner than does curve C, and there is a short period of straight flight before touchdown. The effect of the tighter first turn, caused by better speed control, causes the small differences in the subsequent ground track. This effect is apparently the main factor in producing the better touchdown conditions of case E.

Lateral Guidance Considerations

At the beginning of this paper material was presented that modified the lateral guidance so that initial heading angles greater than $\pi/2$ could be used. An initial condition $\zeta_1 = -1012$ meters, $\zeta_2 = -4000$ meters, $h = 540$ meters, and $\psi_i = \pi$ was selected to demonstrate the adequacy of these changes. As wind and turbulence were used for this check, the heading angle of the velocity vector was less than π radians. As can be seen from figure 11, both the ground track and altitude were good. The landing conditions for this case were not satisfactory, the overshoot was too great, and both ψ and θ were outside of the limits. The poor landing conditions were due to the shallowness of the glide slope, which was about -0.01745 radian at the start of the flare. When the glide slope was increased so that at the start of the flare it was -0.05044 radian, all landing conditions were satisfactory. The glide slope may be increased by increasing the initial altitude or by restricting the letdown until the heading angle is equal to or less than $\pi/2$. The former method was used in this study.

In the landing maneuver shown in figure 11, the turn is simple, that is, the roll angle does not change sign; therefore k_1 for the guidance algorithm (eq. (16)) is determined by the expression

$$k_1 = \left| \frac{\psi_c - \psi_o - k_3 \dot{\psi}_o}{\theta_{AC} - \theta_{AA}} \right|$$

This expression is used for the second calculation of k_1 in appendix B of reference 2.

Avoidance of restricted areas.- In the context of this paper, restricted areas are interpreted as mountains, water towers, buildings, and ground areas over which flight is not permitted. The basic system reported in ref-

erences 1 and 2 and used in this paper was to be used over the last 120 seconds of flight, that is, the final approach and touchdown. During this period it was assumed that all restricted areas would have been passed. However, restricted areas could be handled by assuming that the desired heading angles are supplied from ground control and by using the same turn algorithm (eq. (16)) as normally used for landing approaches. In this case, k_1 is set equal to zero and k_2 is positive. The values of k_1 and k_2 would be maintained until the final approach was started. At this time k_1 would be determined by the method given in appendix B of reference 2 and the sign of k_2 changed so that k_2 is now negative.

Landing maneuver sensitivity to gain k_1.- When the initial position of the airplane is such that $|\zeta_1| \leq |\zeta_2|$ the execution of the landing maneuver is very sensitive to the value of k_1 in equation (16). The sensitivity increases as the wind decreases and is maximum at the zero wind condition. Table II gives the landing conditions for the initial condition $\zeta_1 = \zeta_2 = -4000$ meters, $h = 540$ meters, and $\psi_i = 0.0$ for various values of $k_i(1)$. The value of $k_1(1)$ was specified and the second value was calculated in the usual manner. No wind or turbulence was used in these calculations. In the following discussion two values of k_1 will be referred to $k_1(1)$, the k_1 calculated at the start of the landing maneuver, and $k_1(2)$, the value of k_1 calculated at the completion of the first, that is, as ϕ passes through zero. The points of calculations of these gains are shown on a typical S-curve ground track in figure 12. Inspection of these data (table II) shows that a value $k_1(1)$ between 1.55 and 1.60 gives the best all around landing, whereas for $k_1(1) = 1.75$, a value determined by the guidance algorithm, the heading angle is outside acceptable limits. When k_1 was increased to 1.80, the heading angle was larger and ζ_2 increased from -2.15 meters to -6.08 meters. In neither case has the airplane reached the runway center line; whereas in case G, $k_1(1) = 1.55$, while not reaching the center line was almost centered on the runway. The ground tracks and heading-angle time histories for cases G and K are shown in figure 13. The small value of $k_1(1)$ in case G increases the length of time during the first turn so that the airplane velocity vector is closer to the perpendicular to the runway center line, and when $k_1(2)$ is calculated, it has a smaller value and lengthens the time devoted to the second turn. The total increase in time for case G over case K was 5.7 seconds, enough to give better landing maneuver performance. One way to lengthen the time to land and consequently the length of the ground track without changing the calculated value of $k_1(1)$ is to add the integral of the error to the turn command. When this is done, equation (16) becomes

$$\phi_c = k_2\left[\psi_c - \psi - k_3\dot{\psi} + k_1\left(\theta_{AC} - \theta_{AA}\right)\right] + k_{IG}\int_0^t \left[\psi_c - \psi - k_3\dot{\psi} + k_1\left(\theta_{AC} - \theta_{AA}\right)\right]dt \qquad (20)$$

where k_{IG} is the integrator gain. Case M of table III gives $k_1(1)$, $k_2(2)$, and the landing conditions obtained where an integrator was used. Case M is the same as case K except for the integrator. The gain k_{IG} was set to 0.75 during the interval between points A and B on the ground track

shown in figure 12 and to 0.0 from point B to touchdown. The ground track and heading-angle time history for case M are shown in figure 13. The curves for case M are almost the same as those for case G, as are the landing conditions given in tables II and III. When a wind of -25.8 m/sec at $\pi/4$ radians to the runway center line was included, no integrator was necessary (see case N in table III); however, when the wind was reduced to -12.90 m/sec, case O in table III, an integrator was again necessary. However, only half the amount of gain for the still-air case was required. The value of $k_1(1)$ was about halfway between those for cases G and M. The ground tracks and heading-angle time histories for cases N and O were practically the same as those for case M. From these results it is apparent that the value of k_{IG} is dependent on the value of k_1, which is a function of airplane position and windspeed at the time k_1 is determined, thus making k_{IG} dependent on those quantities. When k_{IG} was determined by the expression

$$k_{IG} = 3.755k_1 - 5.819 \tag{21}$$

satisfactory results were obtained. The gain k_{IG} determined by equation (21) was subject to two limitations: The first is for $k_{IG} \leq 0$, then $k_{IG} = 0.0$; and the second is, if $k_1(2)$ has been calculated, $k_{IG} = 0.0$. The first condition prevents a value of k_1 from being used where an integrator is not needed as in case O of table III. The second condition restricts the use of the integrator to the first turn of the landing trajectory, for example between the points labeled A and B on the ground track of figure 12. Equation (21) was evaluated over a wide range of initial conditions and was found to give satisfactory results.

Equation (21) applies to cases where automatic throttles were used for speed control. A similar problem exists when flaps are used as a speed-control device; however, different constants would have to be used in equation (21).

CONCLUDING REMARKS

The letdown and speed-control subsystem of the longitudinal control system of the possible automatic landing system described in NASA TN D-7611 and NASA TN D-7971 have been studied. In the case of the letdown system a method for constraining the airplane to a letdown in a specified plane is presented. Constraints that control the steepness of the descent path of the original letdown system are also given.

The effectiveness of aerodynamic surfaces instead of automatic throttles as speed-control devices was investigated. In general, drag flaps (speed brakes) or wing flaps provided more precise speed control than the automatic throttles. When the aerodynamic surfaces were used, the vertical touchdown speed was higher than with the automatic throttle, but within the design limits of transport aircraft. Because of less flap activity, wing flaps seem to be preferable to drag flaps.

In addition to the work on the longitudinal control system, modifications to the lateral control system to permit π-radian turns are presented. A method of using integrators to reduce the sensitivity of the lateral guidance system to the gain k_1 (variable gain for the pseudo-radar azimuth-angle error of the turn-control algorithm) in the roll command was developed.

Langley Research Center
National Aeronautics and Space Administration
Hampton, VA 23665
September 17, 1976

APPENDIX A

AUTOMATIC-THROTTLE SPEED-CONTROL SYSTEM

Speed control was achieved through the use of a digital thrust control system. The following equation was used to compute change in thrust ΔT required to eliminate a speed error

$$\Delta T = k_6\left(V_c - V_T\right) - k_{15}m\dot{u} \tag{A1}$$

where

$$k_{15} = 1.0$$

and

$$k_6 = V_c(28.131 + 58.973\delta_f) \tag{A2}$$

If the ΔT calculated by equation (A1) is added to the present thrust T, the new total thrust is $T + \Delta T$. The thrusts T and $T + \Delta T$ were looked up in table I of reference 1, which gave information on how the thrust changed with time. The output of this process was Δt, the time it would take the engine to change its thrust from T to $T + \Delta T$. The change in thrust was added linearly over the time period Δt, so when Δt seconds had passed, the engine thrust was $T + \Delta T$. After the thrust was changed, the thrust controls were shut down for 4 seconds. At the end of 4 seconds, V_T and $\dot{u}$ were sampled to determine whether they were within the control-system dead band. The dead band for V_T was ± 0.1 m/sec and for $\dot{u}$ was ± 0.1 m/sec^2. If the errors were within the dead band, no more changes were made. However, if one or both errors were outside the dead band, thrust changes were made until the error entered the dead bands.

APPENDIX B

FLAP SPEED-CONTROL SYSTEM

The flap control system used for speed control is shown in the following block diagram:

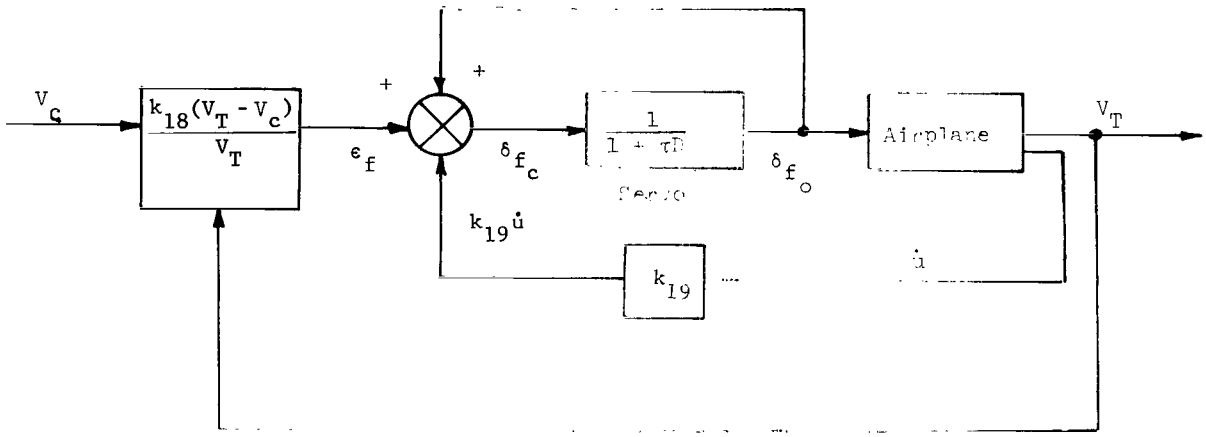

where $k_{18} = 1.461$ and $k_{19} = -0.03$ when wing flaps are used, $k_{18} = 1.190$ and $k_{19} = -0.075$ when drag flaps are used, and $\tau = 0.04$ for both cases.

Flap deflection is positive from the zero flap position. Because ϵ_f represents the estimated change in flap deflection to give the desired speed change, the current position of the servo must be added to ϵ_f to obtain ϵ_{f_c}. The state-variable convolution method was used to perform the integrations in this control system.

TABLE I.- LANDING CONDITIONS FOR SPEED-CONTROL CASES

[Initial condition: ζ_1 = -3000.0 m, ζ_2 = -4000.0 m, h = 540.0 m, ψ_i = 0.0; wind, -25.80 m/sec at $\pi/4$ rad to runway center line; patchy turbulence (see fig. 2)]

Variable \ Case	A (a)	B (b)	C (c)	D (d)	E (e)
ϕ, rad	-6.91×10^{-2}	-6.27×10^{-2}	-1.36×10^{-2}	1.52×10^{-2}	3.23×10^{-3}
ψ, rad	2.08×10^{-2}	1.932×10^{-2}	1.92×10^{-2}	1.32×10^{-2}	-1.52×10^{-3}
ζ_2, m	2.29	1.83	-7.13	-8.93×10^{-2}	9.84×10^{-2}
ζ_1, m	4.83×10^{2}	4.79×10^{2}	-9.544×10^{1}	3.34×10^{2}	2.894×10^{2}
γ, rad	-7.71×10^{-3}	-7.74×10^{-3}	-3.60×10^{-2}	-2.065×10^{-2}	-6.58×10^{-3}
θ, rad	3.55×10^{-2}	4.79×10^{-2}	-7.34×10^{-2}	2.75×10^{-2}	1.66×10^{-2}
w_{z_j}, m/sec	5.32×10^{-1}	5.20×10^{-1}	2.64	1.39	.44
V_T, m/sec	6.895×10^{1}	6.713×10^{1}	7.332×10^{1}	6.736×10^{1}	6.697×10^{1}
t, sec	83.39	84.06	78.63	86.65	86.45

[a]Autothrottle speed control; acceleration feedback gain, 1.0; no wind; no turbulence.

[b]Autothrottle speed control; acceleration feedback gain, 0.45; no wind; no turbulence.

[c]Autothrottle speed control; acceleration feedback gain, 0.45; wind and turbulence.

[d]Drag-flap speed control; acceleration feedback gain, 0.075; wind and turbulence; no thrust cut.

[e]Wing-flap speed control; acceleration feedback gain, 0.01; wind and turbulence; no thrust cut.

TABLE II.- EFFECT OF k_1 ON TOUCHDOWN CONDITIONS

[Initial condition: $\zeta_1 = \zeta_2 = -4000.0$ m, h = 540 m, $\psi_i = 0.0$; no wind or turbulence]

Variable \ Case	F	G	H	I	J	K	L
$k_1(1)$	1.50	1.55	1.60	1.65	1.70	1.75	1.80
$k_1(2)$	1.472	1.52	1.57	1.62	1.67	1.72	1.77
ϕ, rad	2.57×10^{-2}	1.87×10^{-2}	9.34×10^{-3}	3.09×10^{-3}	-2.53×10^{-3}	-4.41×10^{-2}	-6.19×10^{-2}
θ, rad	2.59×10^{-2}	2.42×10^{-2}	1.76×10^{-2}	1.90×10^{-2}	4.42×10^{-2}	4.75×10^{-2}	4.90×10^{-2}
ψ, rad	4.15×10^{-3}	-3.53×10^{-3}	-3.79×10^{-3}	6.37×10^{-4}	8.97×10^{-3}	2.26×10^{-2}	3.93×10^{-2}
ζ_1, m	154.2	126.1	141.5	162.4	53.7	50.1	58.3
ζ_2, m	-3.22	-.842	.474	.724	.444	-2.15	-6.08
γ, rad	-7.14×10^{-3}	-5.75×10^{-3}	-5.52×10^{-3}	-7.20×10^{-3}	-1.53×10^{-3}	-6.83×10^{-3}	-1.09×10^{-2}
V_T, m/sec	69.66	70.18	70.21	68.74	70.04	69.54	69.09
w_{z_j}, m/sec	.497	.403	.388	.495	.107	.475	.753
t, sec	97.1	95.0	93.8	92.8	90.1	89.3	88.5

TABLE III.- EFFECT OF INTEGRATORS IN TURN ALGORITHM

[Initial condition: $\zeta_1 = \zeta_2 = -4000.0$ m, h ▫ 540 m, $\psi_i = 0.0$]

Variable \ Case	M	N	O
Integrator G	0.75	0.0	0.375
$k_1(1)$	1.75	1.58	1.65
$k_1(2)$	1.55	1.55	1.57
ϕ, rad	1.297×10^{-2}	2.33×10^{-2}	1.729×10^{-2}
θ, rad	2.02×10^{-2}	-4.59×10^{-2}	7.34×10^{-3}
ψ, rad	-3.9×10^{-3}	3.038×10^{-3}	2.741×10^{-3}
ζ_1, m	138.7	74.75	52.9
ζ_2, m	-.077	-.493	-.5
γ, rad	-5.89×10^{-3}	-1.26×10^{-2}	-1.087×10^{-2}
V_T, m/sec	70.14	71.94	70.22
w_{z_j}, m/sec	.413	.906	.763
t, sec	94.5	92.2	92.7
Wind, m/sec	0	-25.80	-12.90
Turbulence, m/sec	0	Patchy	0

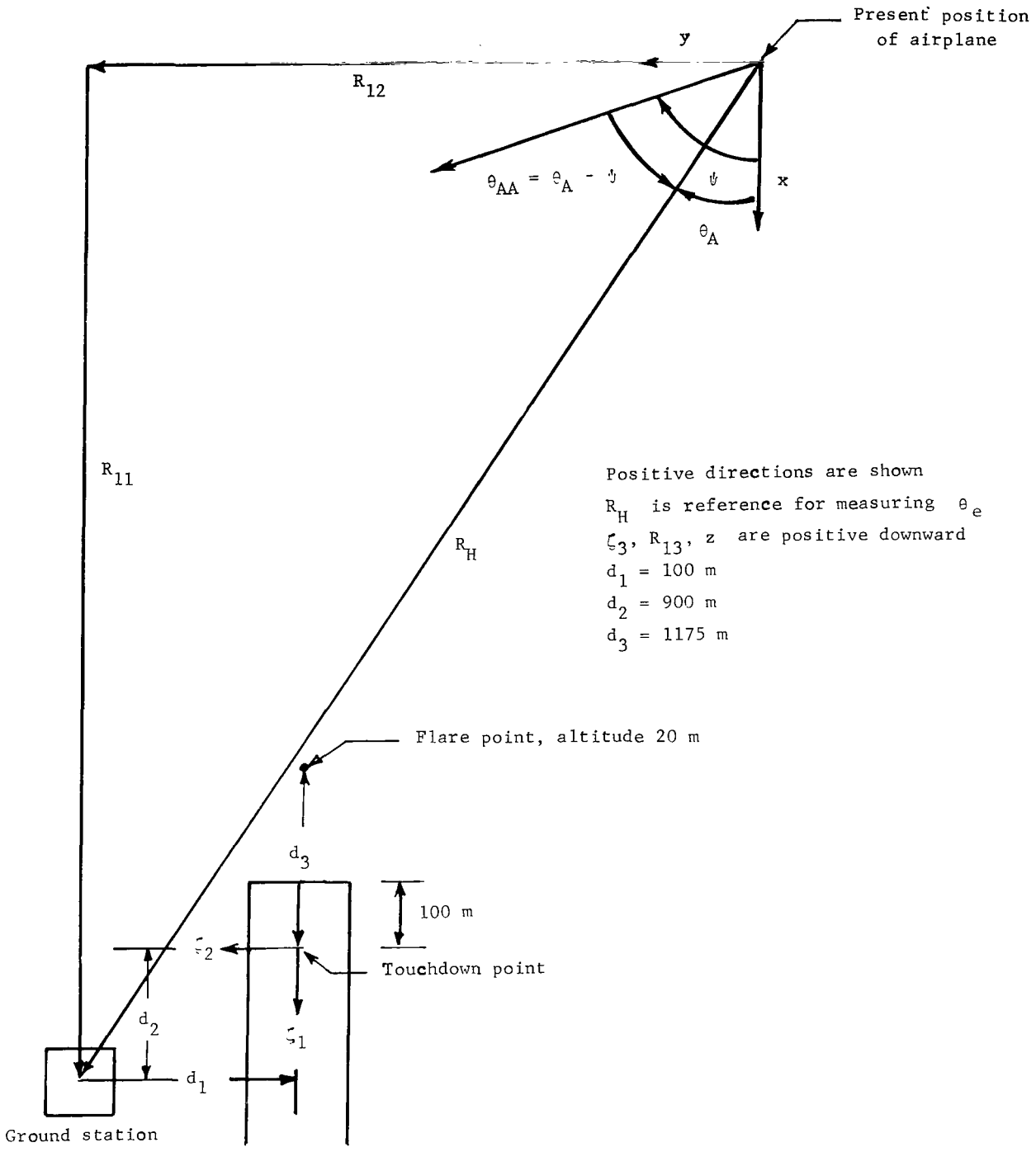

Figure 1.- Geometry used for guidance algorithm inputs.

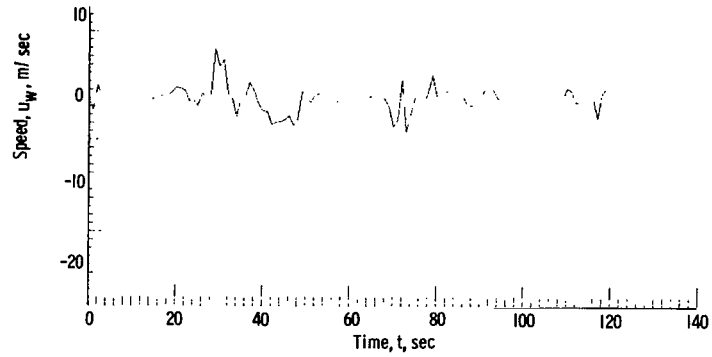

(a) Turbulence along X-axis.

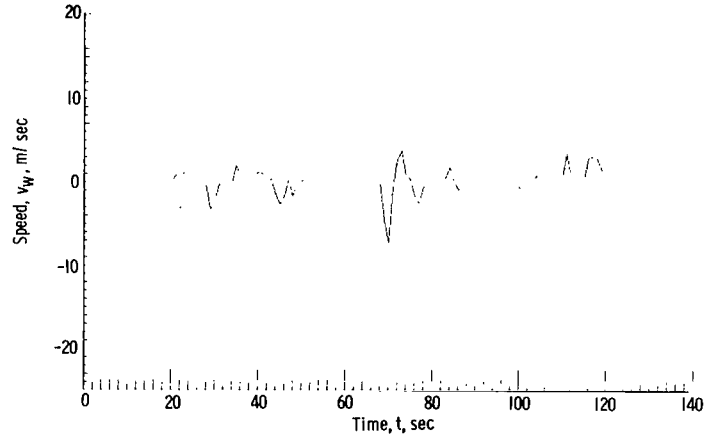

(b) Turbulence along Y-axis.

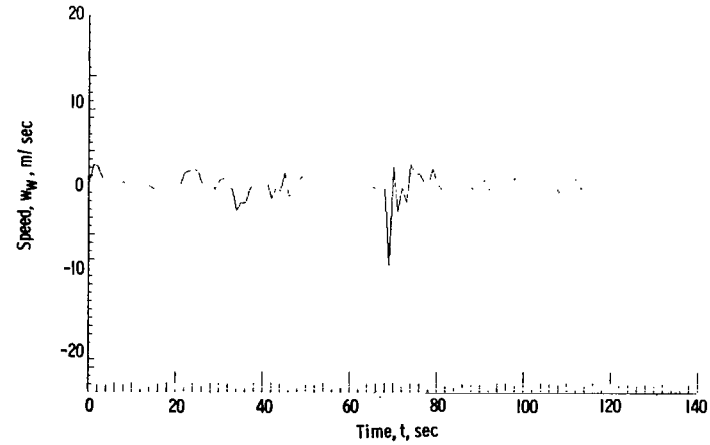

(c) Turbulence along Z-axis.

Figure 2.- Turbulence used in study, referred to as patchy turbulence.

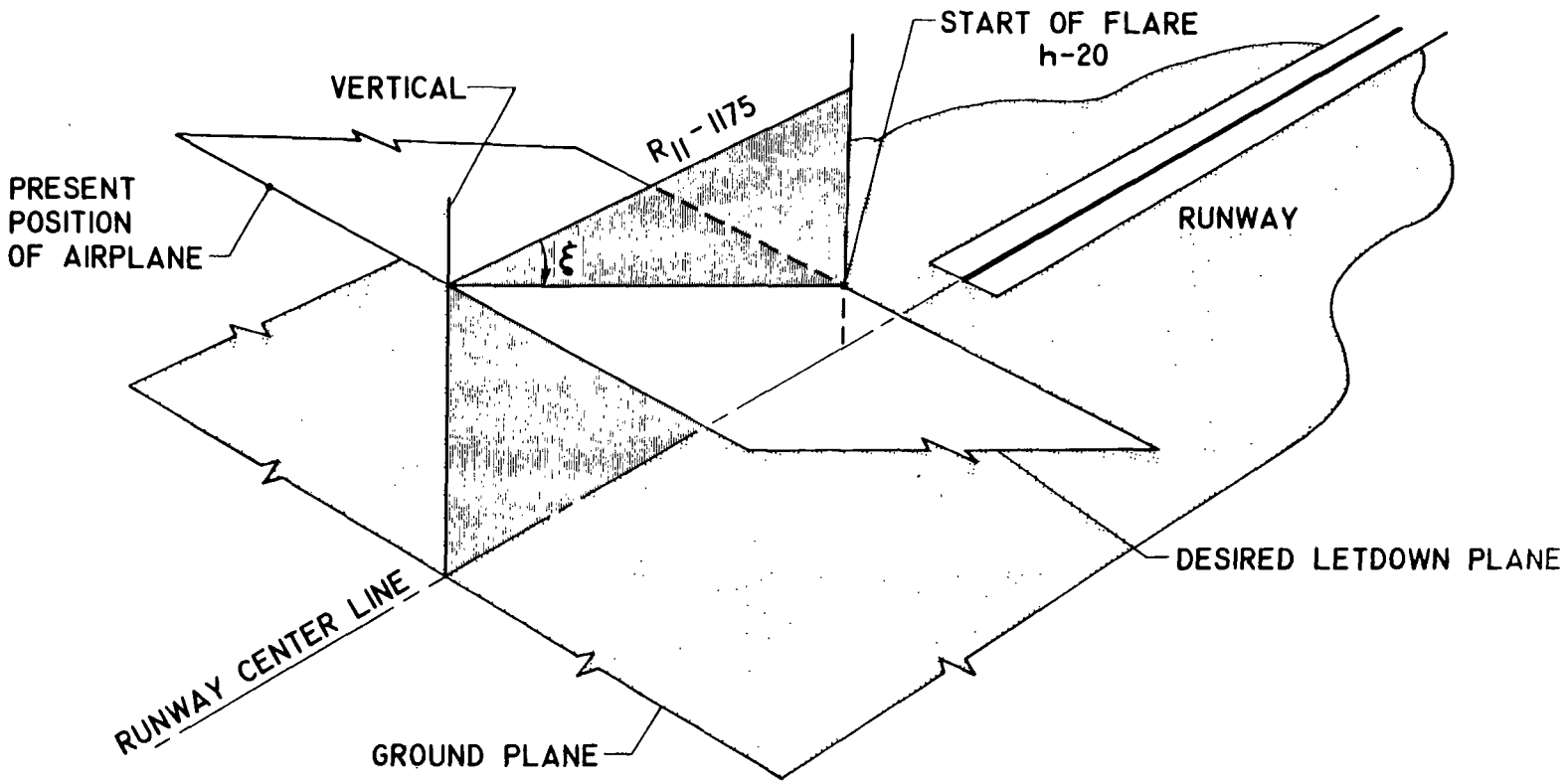

Figure 3.- Geometry used to define flight plane for plane-constrained cases.

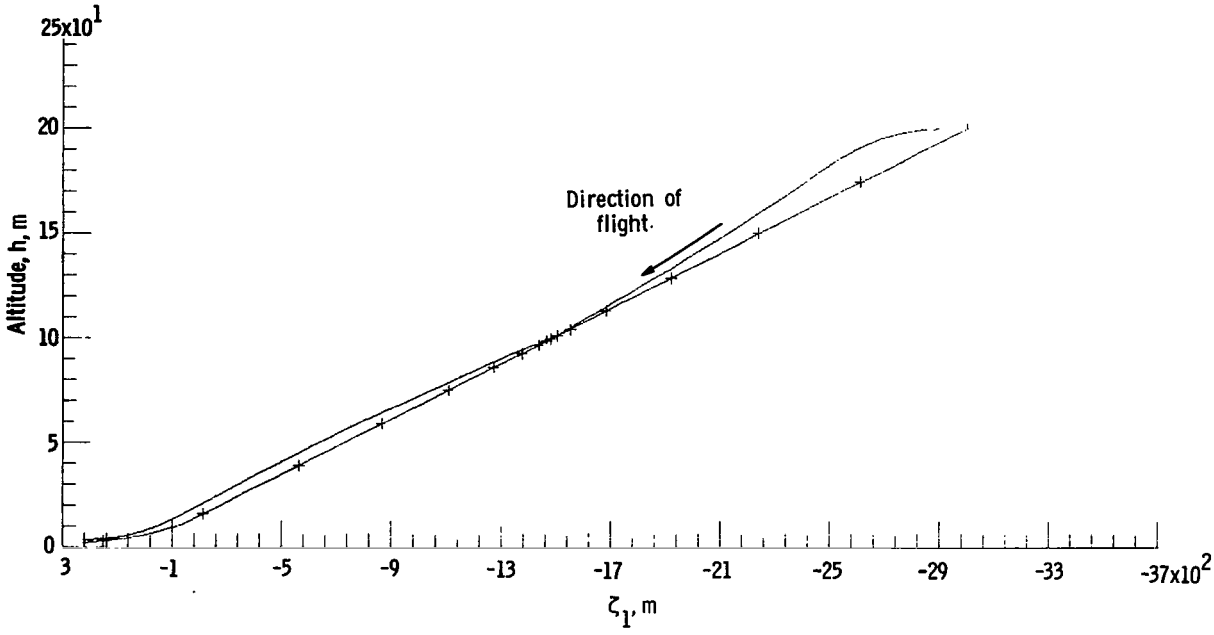

(a) Altitude time history.

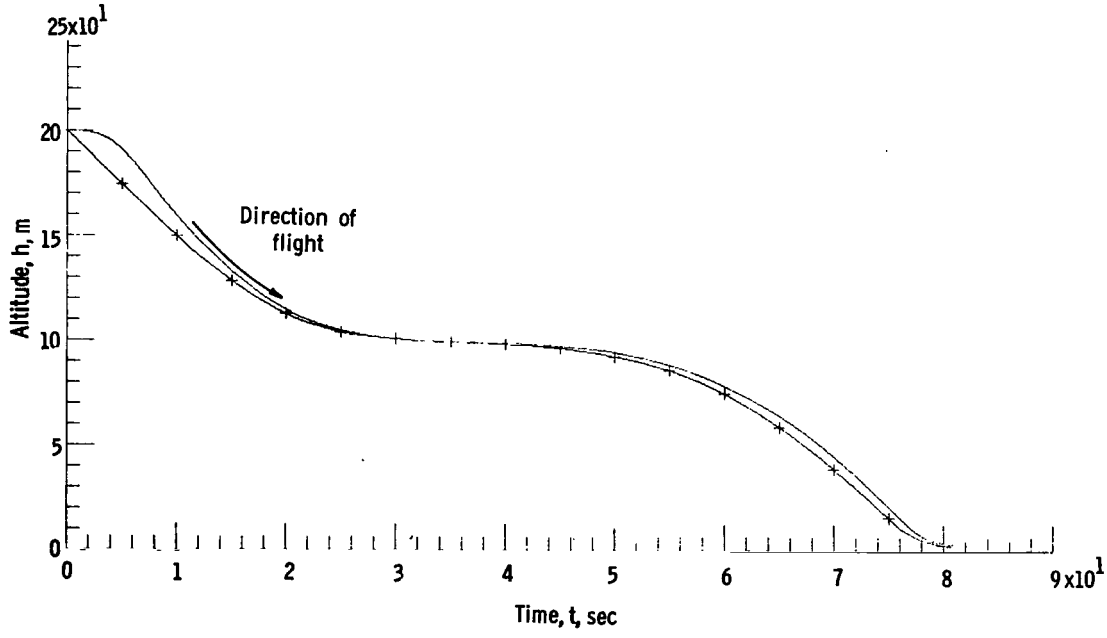

(b) Altitude track.

Figure 4.- Altitude time history, altitude track, and ground track for plane-constrained case; no wind or turbulence. Curve with plus marks is desired flight path; unmarked curve is actual flight path. Plus marks are spaced at 5-sec intervals.

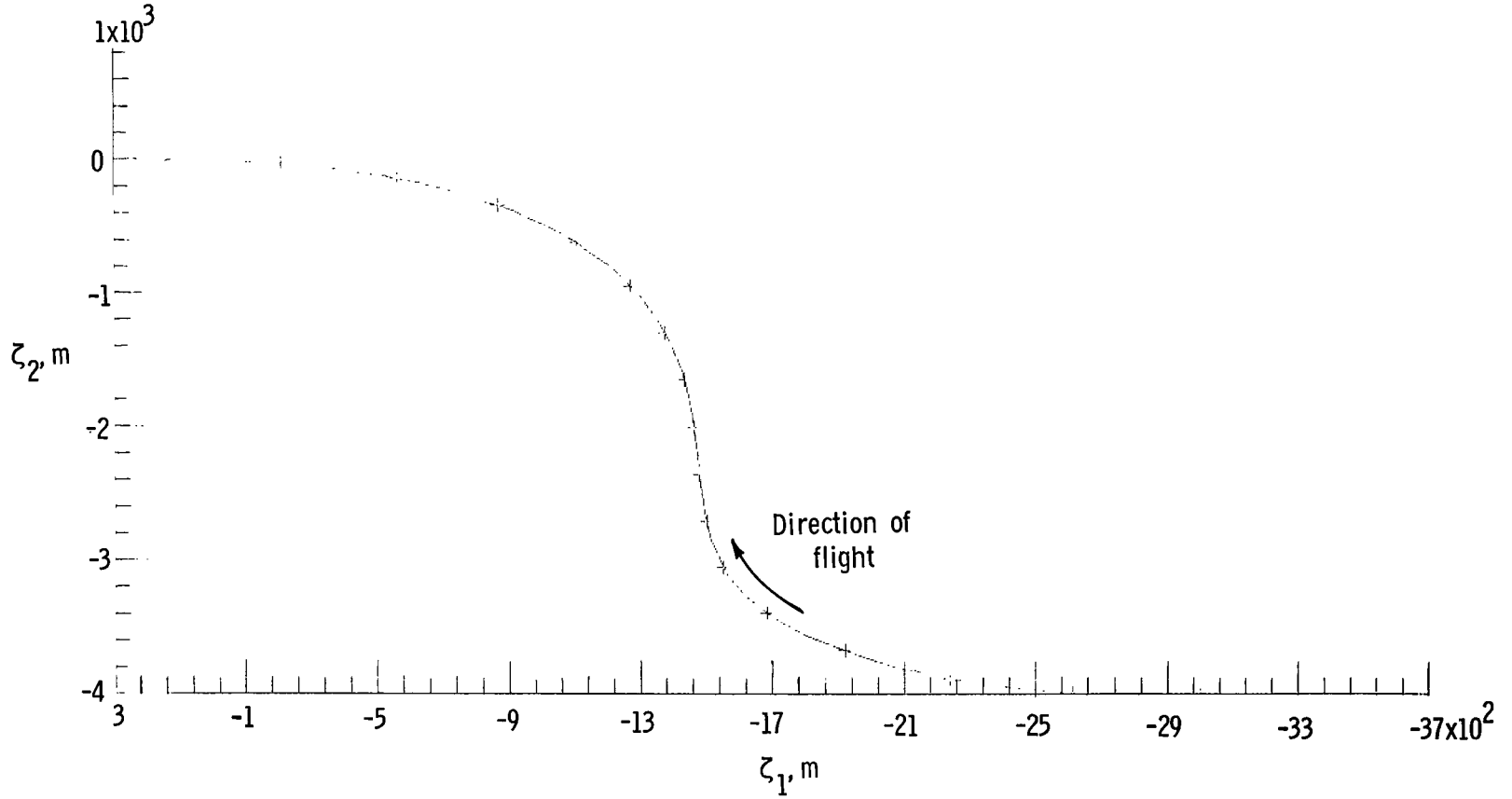

(c) Ground track.

Figure 4.- Concluded.

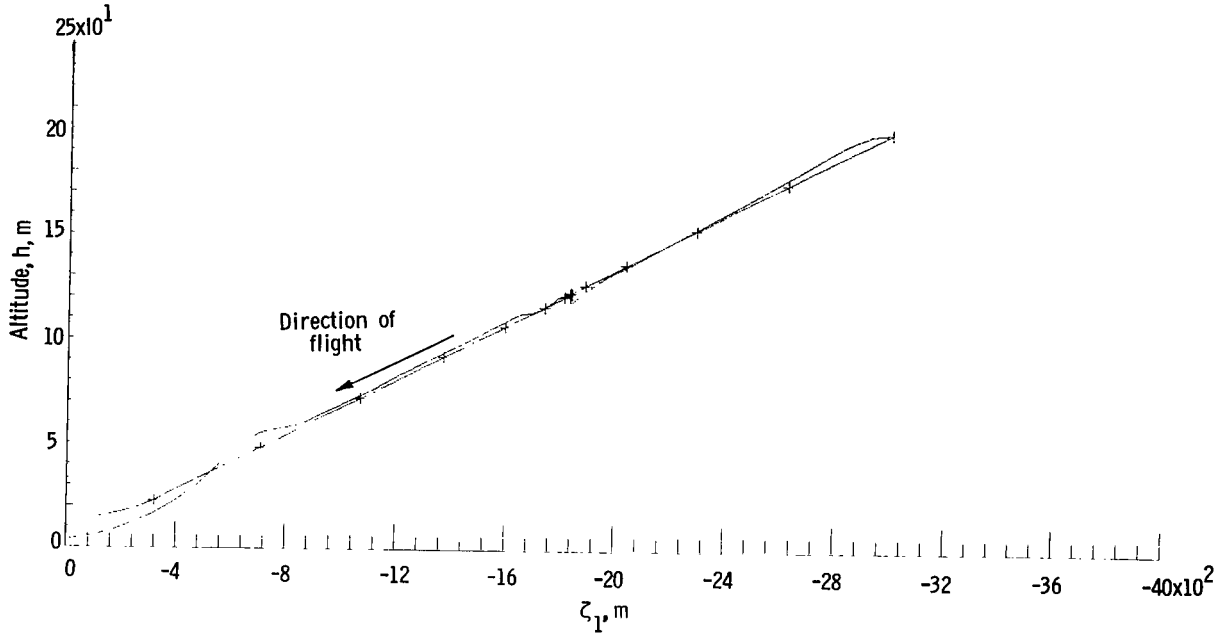

(a) Altitude time history.

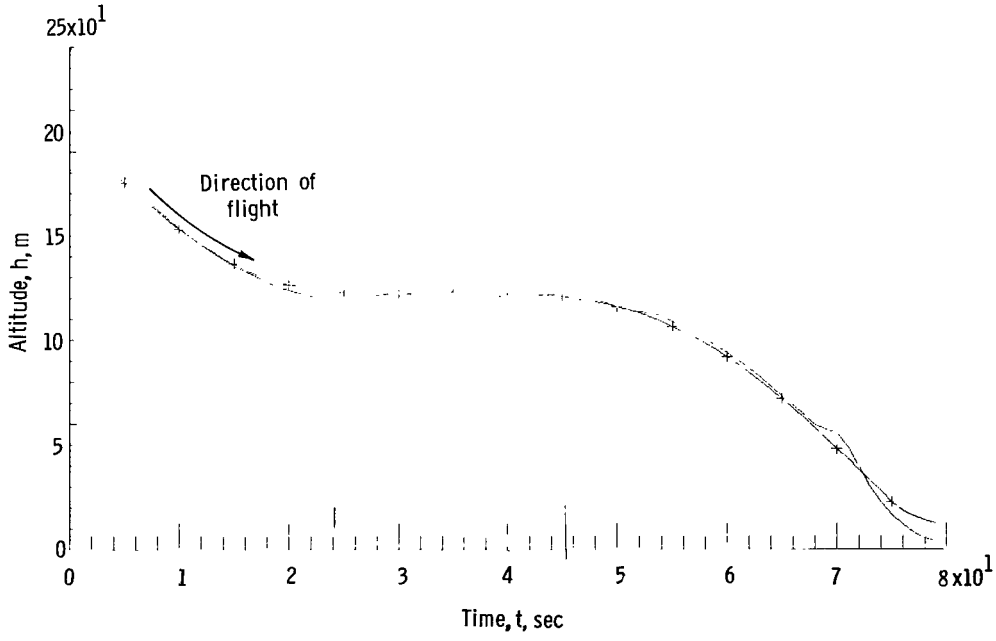

(b) Altitude track.

Figure 5.- Altitude time history and altitude track for plane-constrained case with wind and turbulence.

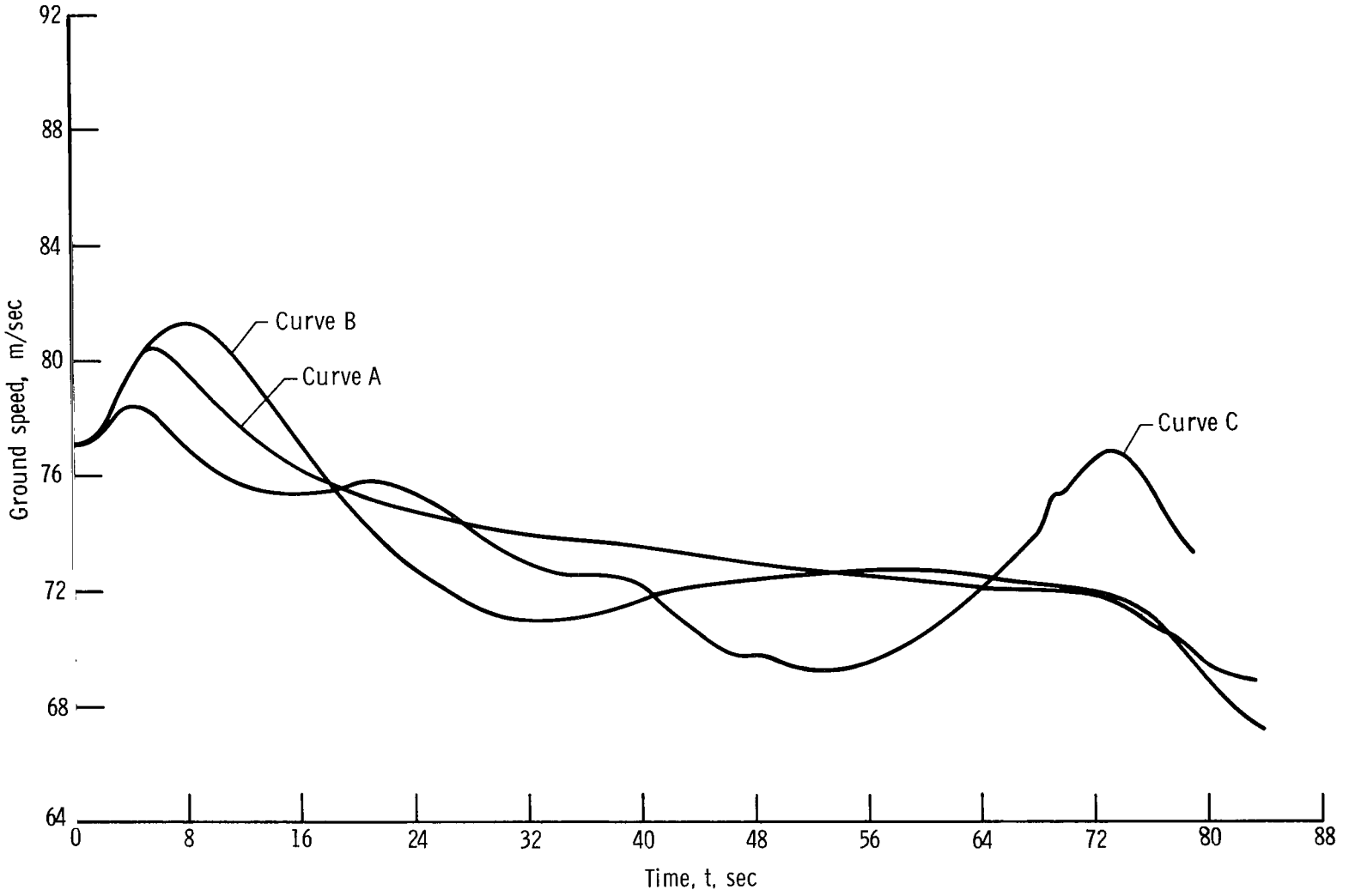

Figure 6.- Time history of speed for automatic-throttle curves A and B; no wind and no turbulence. Curve C; with wind and turbulence.

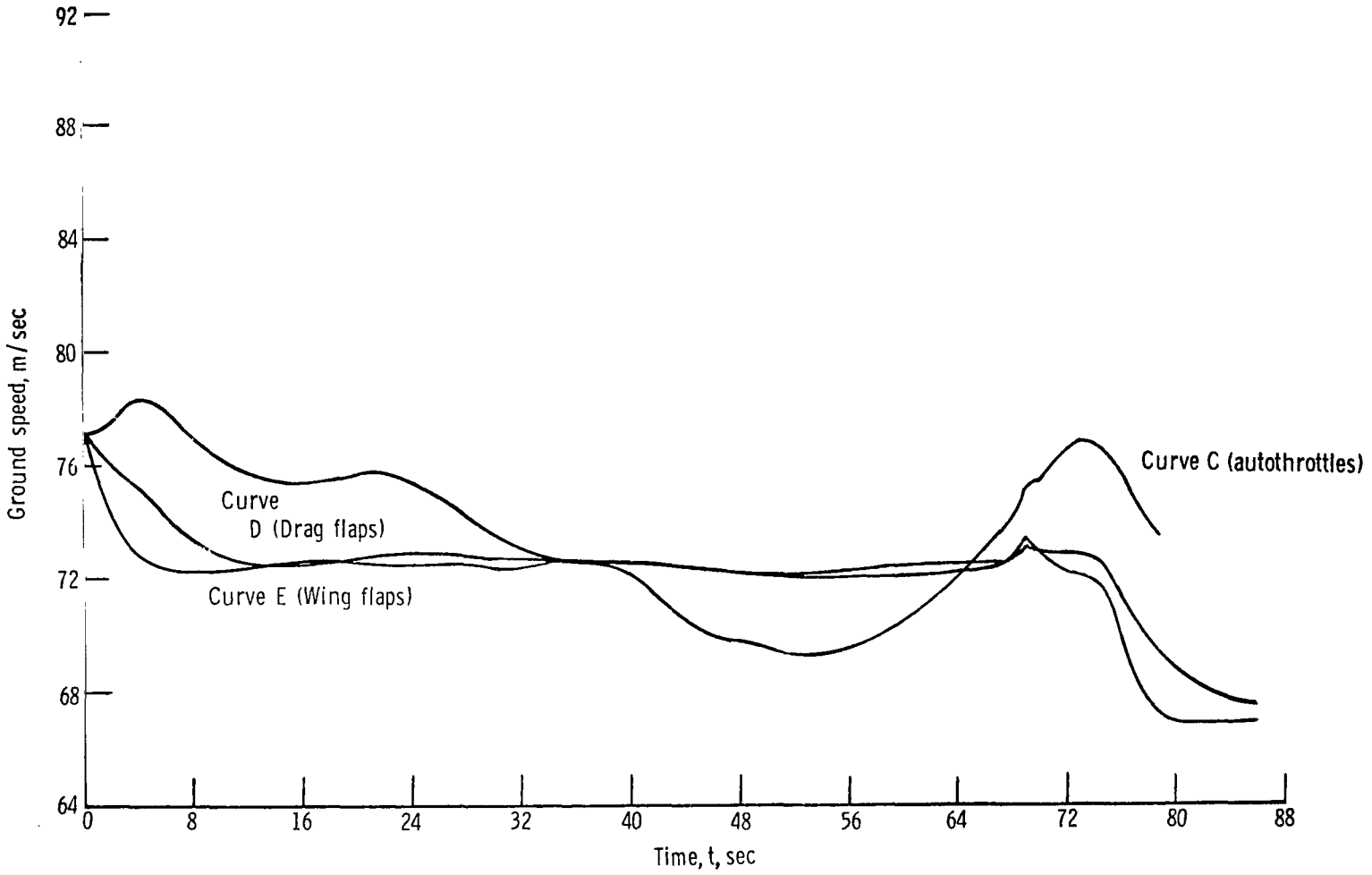

Figure 7.- Comparison of speed control in wind and turbulence for curve C (automatic throttles), curve D (drag flaps), and curve E (wing flaps).

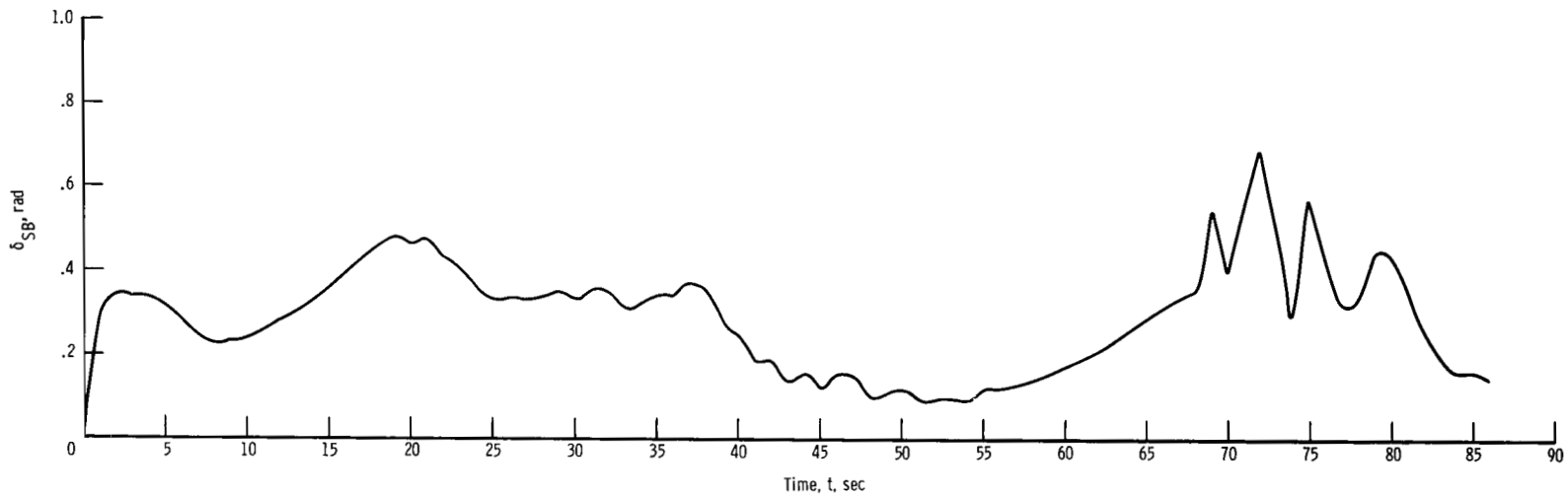

Figure 8.- Time history of speed-brake motion; wind and turbulence used.

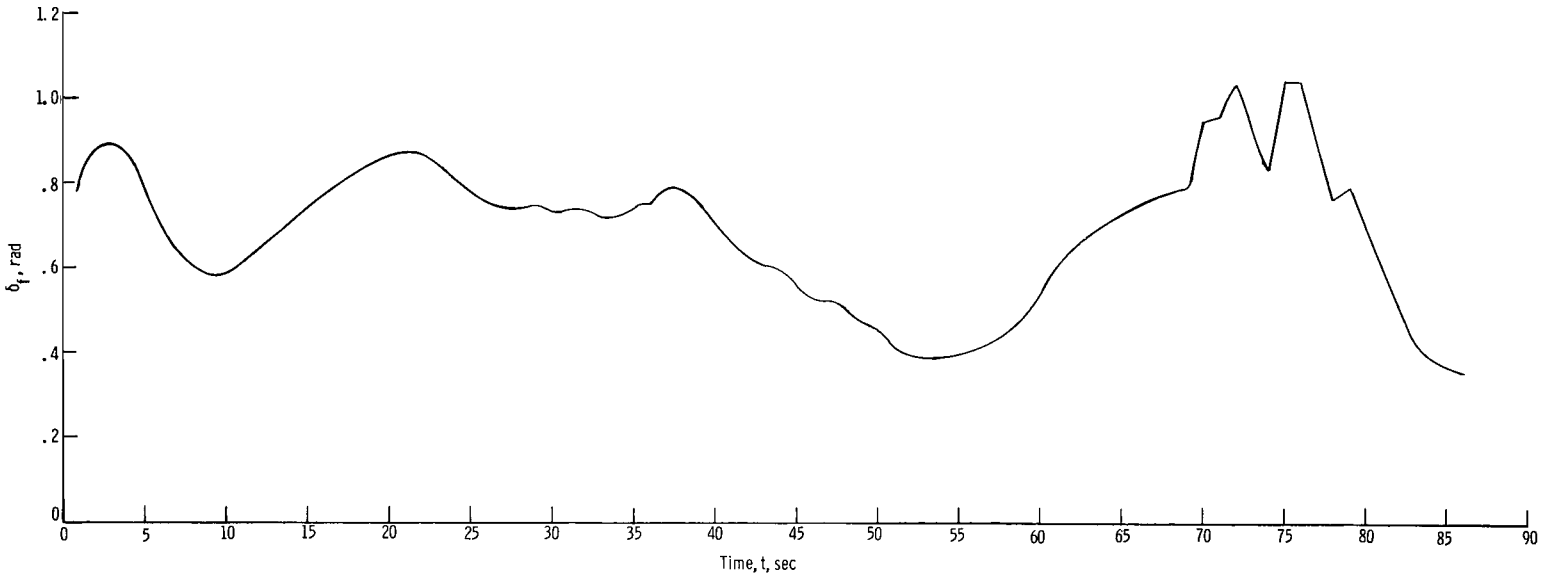

Figure 9.- Time history of wing-flap motion; wind and turbulence used.

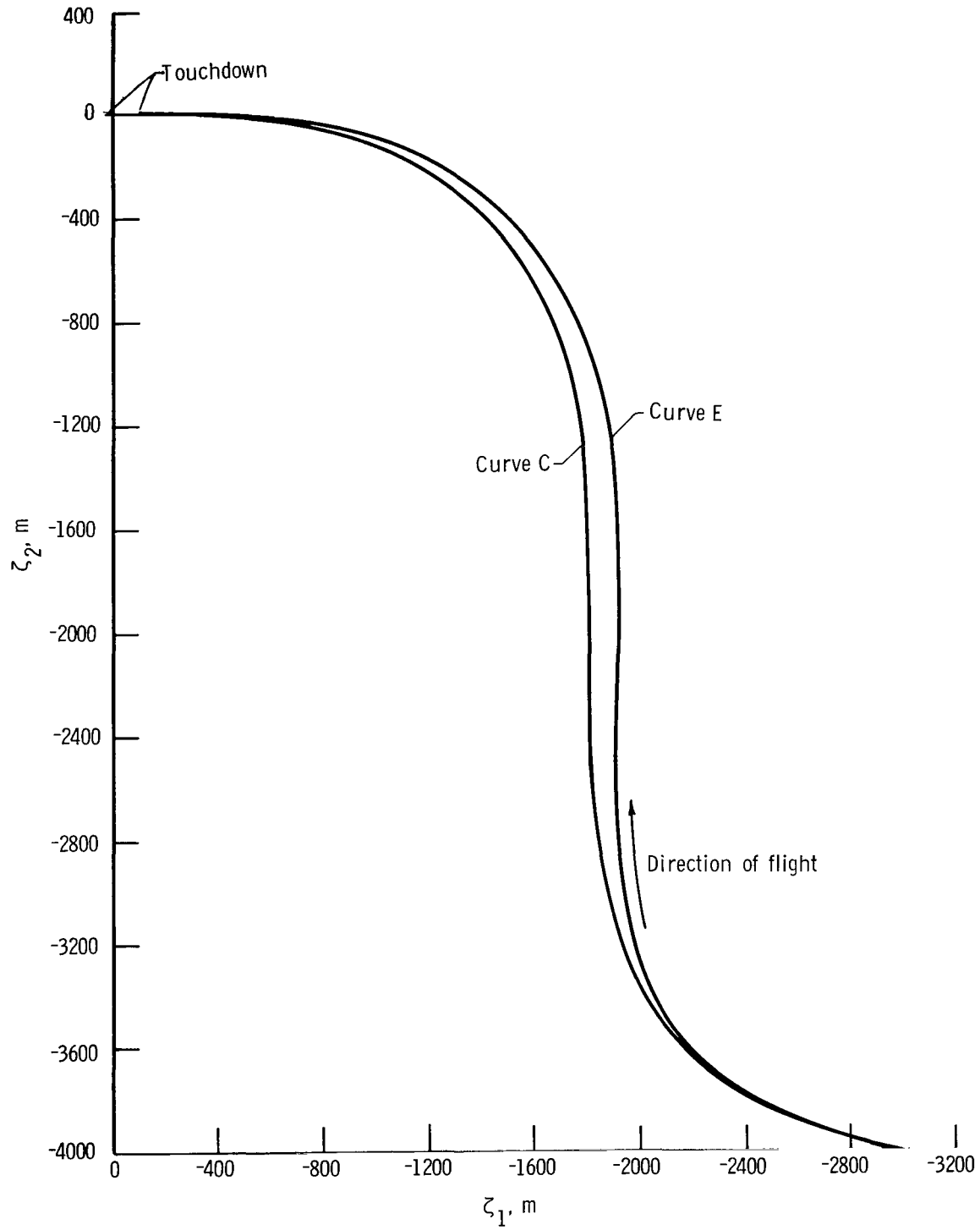

Figure 10.- Effect of speed-control method on ground track in wind and turbulence. Curve C (autothrottle) and curve E (wing flaps).

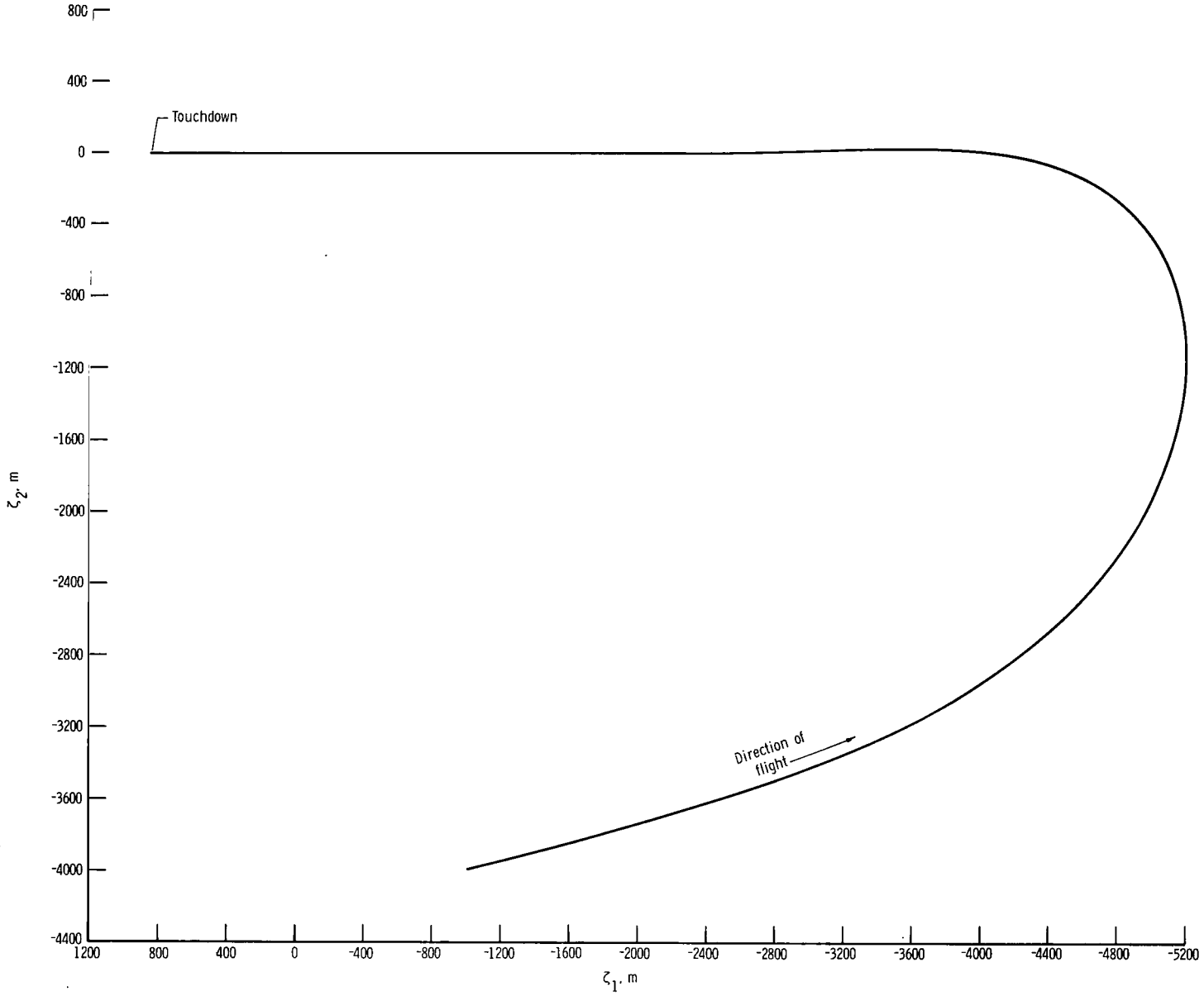

(a) Ground track.

Figure 11.- Landing maneuver when initial heading angle is greater than $\pi/2$ rad.

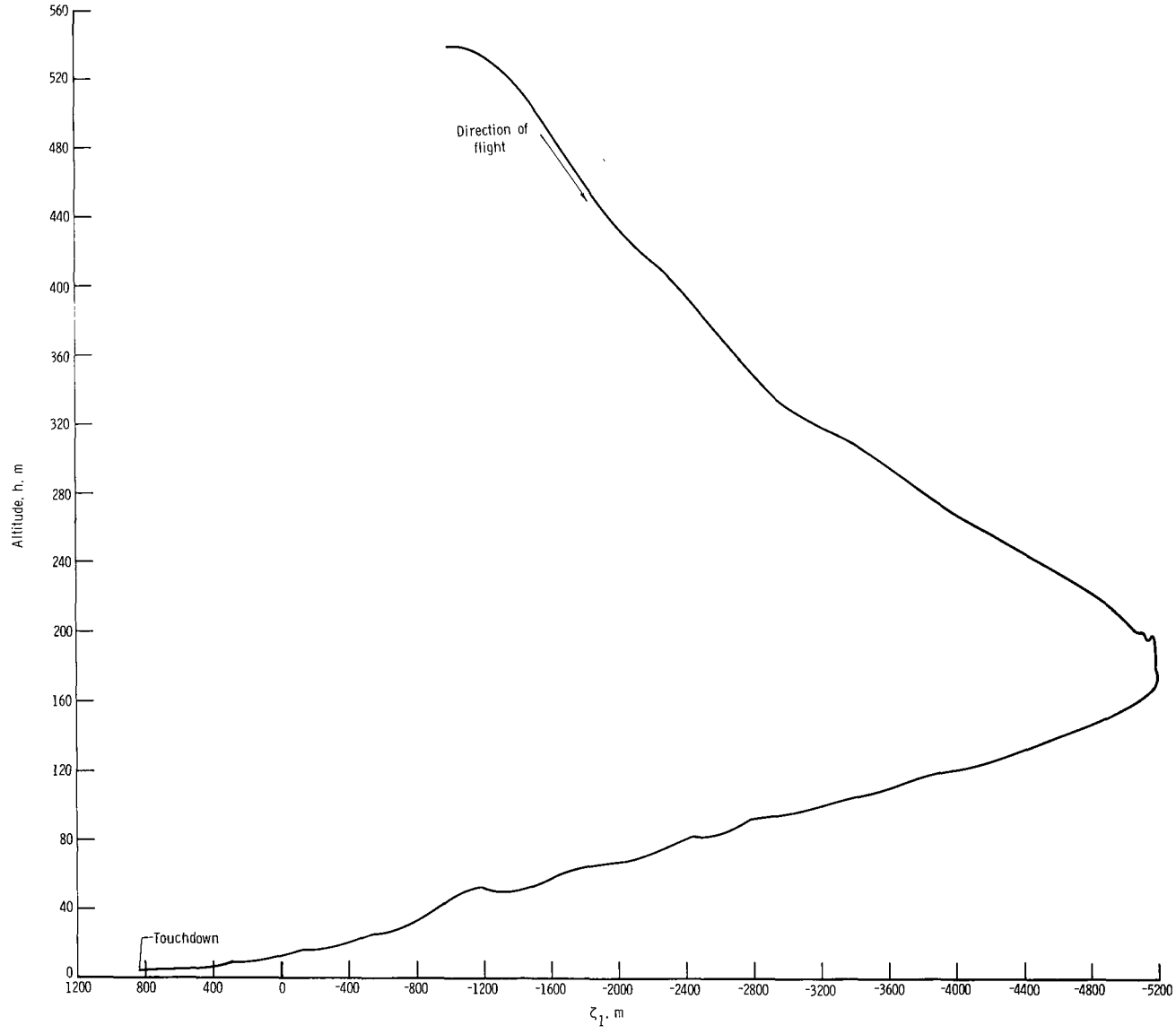

(b) Altitude track.

Figure 11.- Concluded.

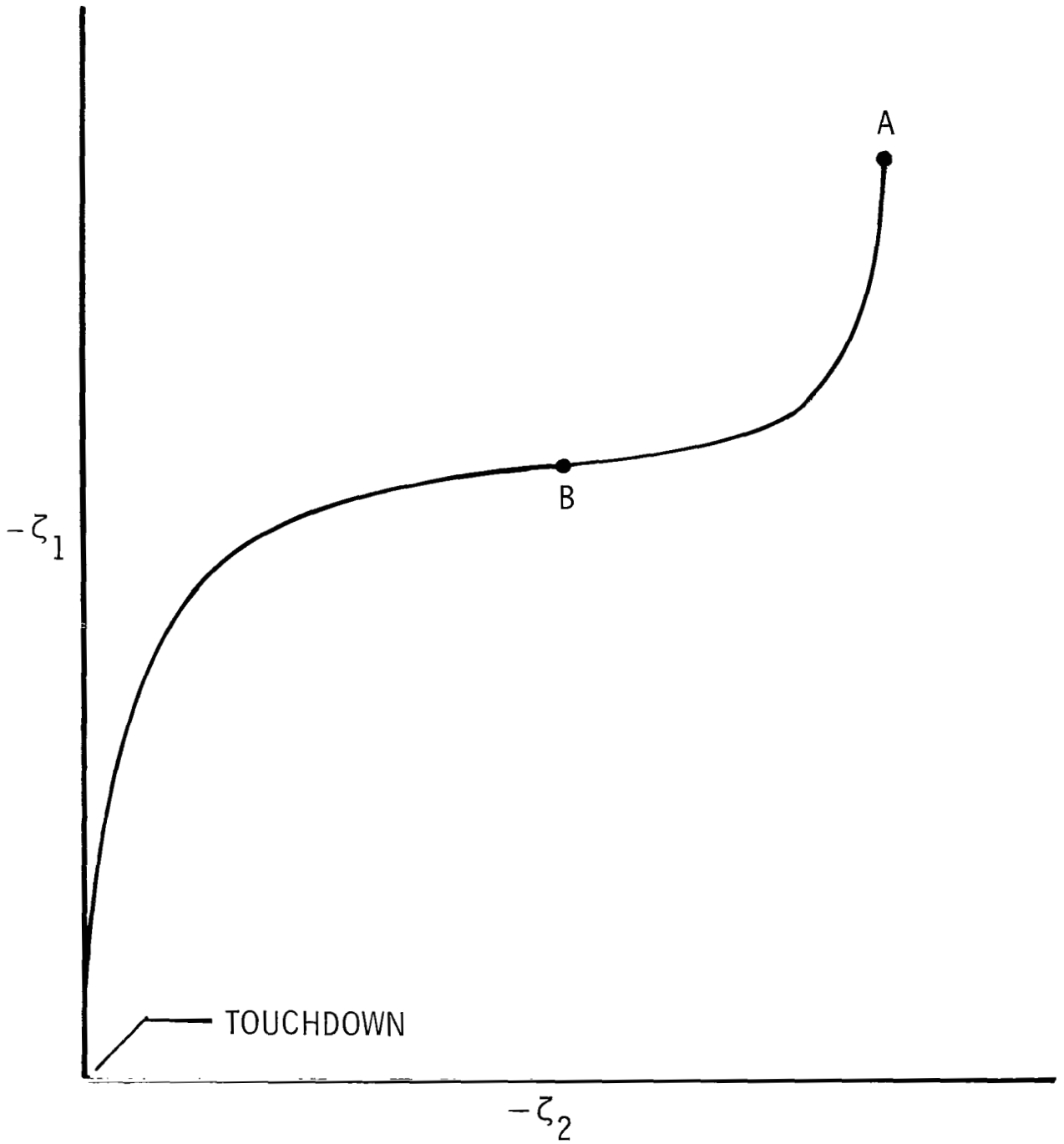

Figure 12.- Typical S-curve ground track. $k_1(1)$ is calculated at A; $k_1(2)$ is calculated at B; at point B, $\phi = 0.0$.

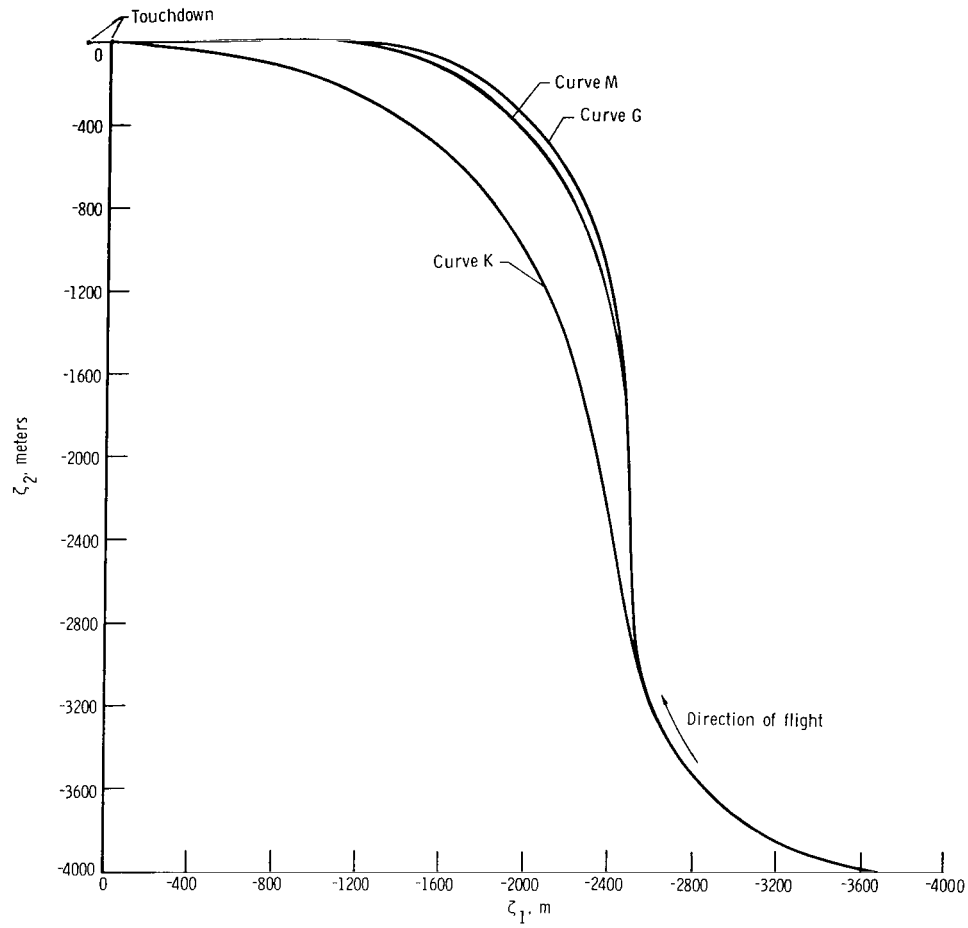

(a) Ground tracks.

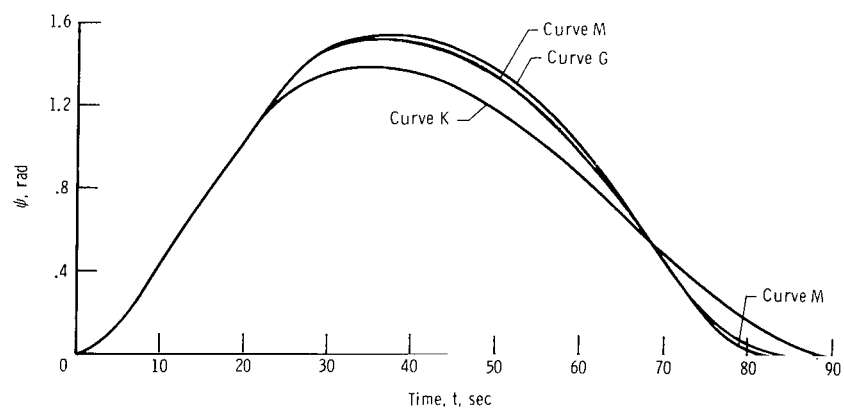

(b) Heading-angle time history.

Figure 13.- Effect of changing gain k_1 on ground track in still air.

914 001 C1 U A 761112 S00903DS
DEPT OF THE AIR FORCE
AF WEAPONS LABORATORY
ATTN: TECHNICAL LIBRARY (SUL)
KIRTLAND AFB NM 87117

"The aeronautical and space activities of the United States shall be conducted so as to contribute . . . to the expansion of human knowledge of phenomena in the atmosphere and space. The Administration shall provide for the widest practicable and appropriate dissemination of information concerning its activities and the results thereof."

—NATIONAL AERONAUTICS AND SPACE ACT OF 1958

NASA SCIENTIFIC AND TECHNICAL PUBLICATIONS

TECHNICAL REPORTS: Scientific and technical information considered important, complete, and a lasting contribution to existing knowledge.

TECHNICAL NOTES: Information less broad in scope but nevertheless of importance as a contribution to existing knowledge.

TECHNICAL MEMORANDUMS: Information receiving limited distribution because of preliminary data, security classification, or other reasons. Also includes conference proceedings with either limited or unlimited distribution.

CONTRACTOR REPORTS: Scientific and technical information generated under a NASA contract or grant and considered an important contribution to existing knowledge.

TECHNICAL TRANSLATIONS: Information published in a foreign language considered to merit NASA distribution in English.

SPECIAL PUBLICATIONS: Information derived from or of value to NASA activities. Publications include final reports of major projects, monographs, data compilations, handbooks, sourcebooks, and special bibliographies.

TECHNOLOGY UTILIZATION PUBLICATIONS: Information on technology used by NASA that may be of particular interest in commercial and other non-aerospace applications. Publications include Tech Briefs, Technology Utilization Reports and Technology Surveys.

Details on the availability of these publications may be obtained from:

SCIENTIFIC AND TECHNICAL INFORMATION OFFICE

NATIONAL AERONAUTICS AND SPACE ADMINISTRATION

Washington, D.C. 20546